Task D/CCFR-NuTeV/MINERvA

(CCFR/NuTeV = FNAL Tevatron Experiments E744/E770/E815, NUMI-MINERvA = near detector neutrino detector at FNAL)

A. Current Participants of the Rochester CCFR-NuTeV Group during 2003-2003

Faculty: Prof. Arie Bodek, Prof. Kevin McFarland,
(Prof. Steve Manly, Collaborating Faculty on MINERvA)
Research Faculty: Dr. Pawel de Barbaro, Dr. Howard Budd, and
Dr. Willis K. Sakumoto
Previous Participants: U. K. Yang, S. Avvakumov (PhD Students)

Introduction

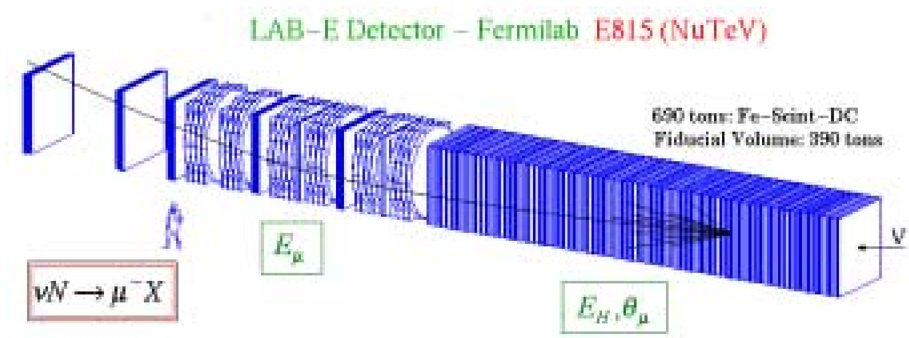

Figure 1: The CCFR/NuTeV Detector

The NuTeV experiment combined an upgraded CCFR detector (shown in Figure 1), a new continuous hadron calibration beam, and a new SSQT neutrino beam. The new SSQT neutrino beam was sign-selected, thus allowing neutral current data to be taken separately with neutrinos and antineutrinos. The upgraded detector had new liquid scintillator and new phototubes. Upstream of the detector is a large volume filled with helium bags. It is a decay channel used in a search for neutral heavy leptons. The main physics goal of NuTeV is an improved measurement of the electroweak mixing angle by using separate neutrino and antineutrino beams.

CCFR/NuTeV Highlights for 2002-2003

1. Structure Function Analysis

   The University of Rochester is working with the University of Pittsburgh on the NuTeV structure function analysis. This is a continuation of the work by Rochester Ph.D. student Un-ki Yang and Professor Arie Bodek. The Rochester group used CCFR data to perform the following structure function measurements: differential cross sections vs x y and E_ν, F_2, $\Delta xF_3 = xF_3^\nu$-$xF_3^{\overline{\nu}}$, and $R^\nu = \sigma_L/\sigma_T$. These were significant improvements to our knowledge of structure functions and parton distributions. (Note, additional work on structure functions by Yang and Bodek included analysis of electron, muon and neutrino scattering, and CDF W asymmetry data).

Dr. Un-Ki Yang received the Universities Research Association (URA) award for the best Fermilab thesis of 2001-2002. Note that this is the second year in a row that a Rochester PhD student received this URA Award. In addition, the Association of Korean Physicists in America presented a citation of Honorable Mention for the 2001 Outstanding Young Researcher Award to Dr. Un-Ki Yang for his truly outstanding scholarly and pioneering research in high energy physics. Yang was also awarded the Lobkowicz prize for best Ph.D. thesis in high energy physics in the department of physics and astronomy at the University of Rochester in 2001.

The sum of ν_μ and $\overline{\nu}_\mu$ differential cross sections for charged current interactions on isoscalar target is related to the structure functions as follows:

$$\left[\frac{d^2\sigma^\nu}{dxdy} + \frac{d^2\sigma^{\overline{\nu}}}{dxdy}\right]\frac{(1-\epsilon)\pi}{y^2G_F^2ME_\nu} = 2xF_1[1+\epsilon R] - \frac{y(1-y/2)}{1+(1-y)^2}\Delta xF_3.$$

Here G_F is the weak Fermi coupling constant, M is the nucleon mass, E_ν is the incident energy, the scaling variable $y = E_h/E_\nu$ is the fractional energy transferred to the hadronic vertex, E_h is the final state hadronic energy, and $\epsilon \simeq 2(1-y)/(1+(1-y)^2)$ is the polarization of virtual W boson. The structure functions $2xF_1$, R, and ΔxF_3 can be extracted from the measurements of $\frac{d^2\sigma^\nu}{dxdy}$ and $\frac{d^2\sigma^{\overline{\nu}}}{dxdy}$ at various values of ϵ. The structure function $2xF_1$ is expressed in terms of F_2 by $2xF_1(x,Q^2) = F_2(x,Q^2) \times \frac{1+4M^2x^2/Q^2}{1+R(x,Q^2)}$, where Q^2 is the square of the four-momentum transfer to the nucleon, $x = Q^2/2ME_h$ (the Bjorken scaling variable) is the fractional momentum carried by the struck quark, and $R = \sigma_L/\sigma_T$ is the ratio of the cross-section of longitudinally to transversely-polarized W-bosons. The term $\Delta xF_3 = xF_3^\nu$-$xF_3^{\overline{\nu}}$ in leading order is $\simeq 4x(s-c)$.

Structure function measurements from NuTeV have several advantages over CCFR measurements. Three of these advantages are stated below:

- During the planning stage of NuTeV, Prof Arie Bodek conceived of the continuous hadron and muon calibration beam. In CCFR, the calibration beam entered the side of the building, and we had to move the detector and disrupt data taking to do calibrations. The hadron beam line was modified and redirected at the cener of the building. NuTeV ran the calibration beam concurent with neutrino data taking. The Rochester group analyzed the hadron energy calibration data which resulted in a smaller error of 0.43% (versus 1.0% in CCFR.

- Since the beam is sign selected, even events for which the final state muon is not analyzed by the toroid spectrometer can be used in structure function analysis (because of the separate running in ν and $\overline{\nu}$ modes). These "range outs" extends the range to high y and low ϵ.
- Since the sign selected beam creates either ν or $\overline{\nu}$, the final state muons are always focused toward the center of the muon spectrometer. This results in higher acceptance for high y events with low energy final state muons.

Preliminary versions of the cross sections and structure functions, F_2, xF_3, and R exist. Figure 2 shows the NuTeV preliminary $F_2(x,Q^2)$. We see agreement with the previous ν-Fe measurements. In addition, we see good agreement with the NLO QCD curve. The preliminary measurement of R and xF_3 show good agreement with the previous CCFR measurement.

The plan is to finalize values of the cross section and structure functions in 2003. The NuTeV "range-out" data, which measure the structure functions at high y, will be added to the sample. This will give a better $2xF_1$ R fit. The QCD analysis which CCFR performed will be done on the NuTeV structure functions. This includes the QCD fits and extraction of α_s.

2. Precision Determination of $\sin^2\theta_W$

Professor Kevin McFarland has been leading the CCFR and NuTeV analysis of $\sin^2\theta_W$.

Neutrino-nucleon scattering is one of the most precise probes of the weak neutral current. The ratio of neutral current (NC) to charged current (CC) cross-sections for either ν or $\overline{\nu}$ scattering from isoscalar targets of u and d quarks can be written as:

$$R^{\nu(\overline{\nu})} \equiv \frac{\sigma(\overset{(-)}{\nu} N \to \overset{(-)}{\nu} X)}{\sigma(\overset{(-)}{\nu} N \to \ell^{-(+)} X)} = (g_L^2 + r^{(-1)} g_R^2),\ \text{where } r \equiv \frac{\sigma(\overline{\nu}N \to \ell^+ X)}{\sigma(\nu N \to \ell^- X)} \sim \frac{1}{2},$$

where $g_{L,R}^2$ are the average effective left and right-handed ν-quark coupling. Charm production, which affects CC cross-sections, is a major theoretical uncertainty. Hence, NuTeV measures the Paschos-Wolfenstein variable

$$R^- \equiv \frac{\sigma(\nu_\mu N \to \nu_\mu X) - \sigma(\overline{\nu}_\mu N \to \overline{\nu}_\mu X)}{\sigma(\nu_\mu N \to \mu^- X) - \sigma(\overline{\nu}_\mu N \to \mu^+ X)} = \frac{R^\nu - rR^{\overline{\nu}}}{1-r} = (g_L^2 - g_R^2) = \frac{1}{2} - \sin^2\theta_W.$$

Measuring R$^-$ required a new beam line to create separate ν and $\overline{\nu}$ beams. In addition, this new beam reduces the uncertainty of the other major systematic error, the ν_e contamination. The continuous calibration of the detector reduces the detector related systematic errors.

NuTeV measures the ratio of short to long events in the ν and $\overline{\nu}$ beams to be:

$$R^\nu_{\text{exp}} = 0.3916 \pm 0.0007 \text{ and } R^{\overline{\nu}}_{\text{exp}} = 0.4050 \pm 0.0016.$$

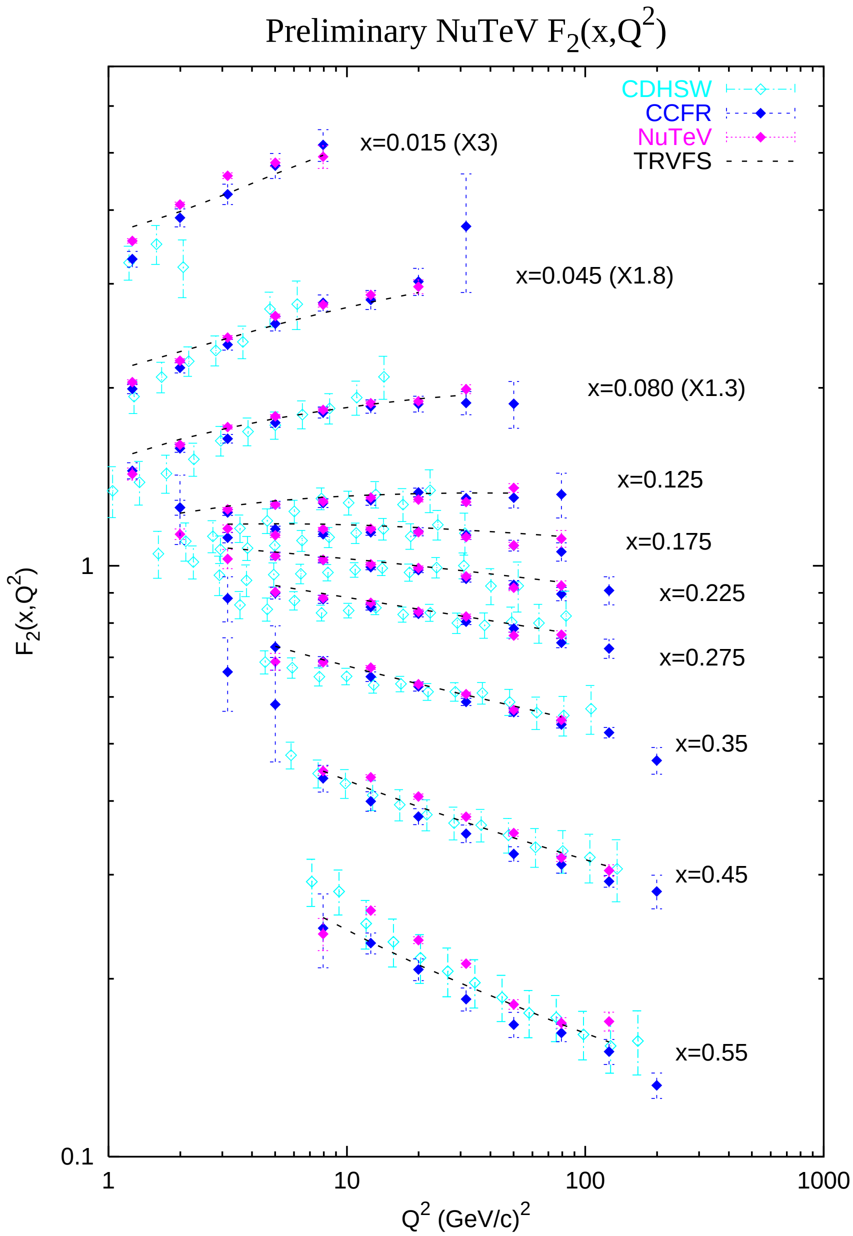

Figure 2: NuTeV preliminary $F_2(x, Q^2)$. NLO curve is TR-VFS with MRTS99 (Thorne & Roberts Phys.Lett B421,303(1998)

A detailed leading order (LO) Monte Carlo program converts $R^{\nu}_{\rm exp}$and $R^{\overline{\nu}}_{\rm exp}$to $\sin^2\theta_W$. This yields: $\sin^2\theta_W^{\rm (on-shell)} = 0.2277 \pm 0.0016$, assuming M_{top}=175 GeV and M_{Higgs}=150 GeV. This is in very good agreement with the world average of all previous neutrino experiments of $\sin^2\theta_W = 0.2277 \pm 0.0036$ (but the NuTeV errors are smaller). The leading terms in the one-loop electroweak radiative corrections produce the small residual dependence of our result on M$_{top}$ and M$_{Higgs}$. The Standard Model fit to all other electroweak measurements excluding neutrino experiments gives $\sin^2\theta_W = 0.2227 \pm 0.00037$, approximately 3σ from the NuTeV result.

The NuTeV results has generated a great deal of interest. If new physics is the explanation, then the NuTeV result requires new tree level physics which are difficult to accomplish with "natural" models beyond the Standard Model. Hence, much of the discussion on the NuTeV anomaly has been on Standard Model explanations. Our recent efforts have been devoted to understanding the conventional explanations for the 3 σ deviation from the Standard Model. These include the NLO and NNLO QCD corrections, PDF uncertainties, charm uncertainties, isospin breaking effects, and nuclear effects. Many of these effects are very small for R^-. However, NuTeV does not measure R^-. R^- is the ratio of cross sections, while NuTeV measures the ratio of experimental events with cuts. The difference between R^- and NuTeV's measurement includes experimental cuts (E_{had}), backgrounds, cross talk between NC and CC, different NC and CC acceptance, charm production, etc.

The QCD corrections to DIS neutrino scattering for NLO and NNLO are known. The Paschos-Wolfenstein ratio can be written to include these higher order terms. We use this result to get a NLO QCD correction to R^-_{model}=-0.00033 (about $1/4\sigma$ closer to the SM prediction). This correction includes the y-cut from the 20 GeV E_had cut and an effective high y-cut from being unable to see very low energy muons in CC events.

It has been suggested that the NuTeV results can be explained by an asymmetric strange sea, i.e. if $\langle s(x)\rangle \neq \langle \overline{s}(x)\rangle$. However, this has been ruled out in our recent publication, PRD 65:111103,2002 (hep-ex/0203004). Here we use the NuTeV opposite sign dimuon measurement to extract $\langle S\rangle - \langle\overline{S}\rangle = -0.0027 \pm 0.0013$. Instead of explaining the NuTeV results, our measurement of the strange sea asymmetry results in an increase in the NuTeV value of $\sin^2\theta_W$, $\Delta\sin^2\theta_W = +0.0020 \pm 0.0009$, which increases the discrepancy with respect to Standard Model expectation to 3.7σ. The asymmetric strange sea comes from CDHSW structure functions. The CDHSW structure functions deviate from the QCD prediction at high x, and an asymmetric strange sea is given as an explanation. The CCFR structure functions are consistent with QCD and do not claim to see asymmetric strange sea. A preliminary analysis of the s and $\overline{s}$ asymmetry in an NLO cross-section model finds the momentum carried by the seas are consistent within uncertainties.

To best answer these and other questions, we are building a full NLO ν DIS event generator. We do not believe this will be a big effect. This is a calculation to order α_s based on a 1978 paper of Altarelli, Ellis, Martinelli. As R_L is included in our Monte Carlo program, we only need to include corrections to xF_3. The plan will be to do light quarks first and then put in NLO charm production. A NuTeV thesis topic (D. Mason, University of Oregon) is a NLO analysis of charm production, which includes NLO study of the strange sea. This code will included in our Monte Carlo program for $\sin^2\theta_W$.

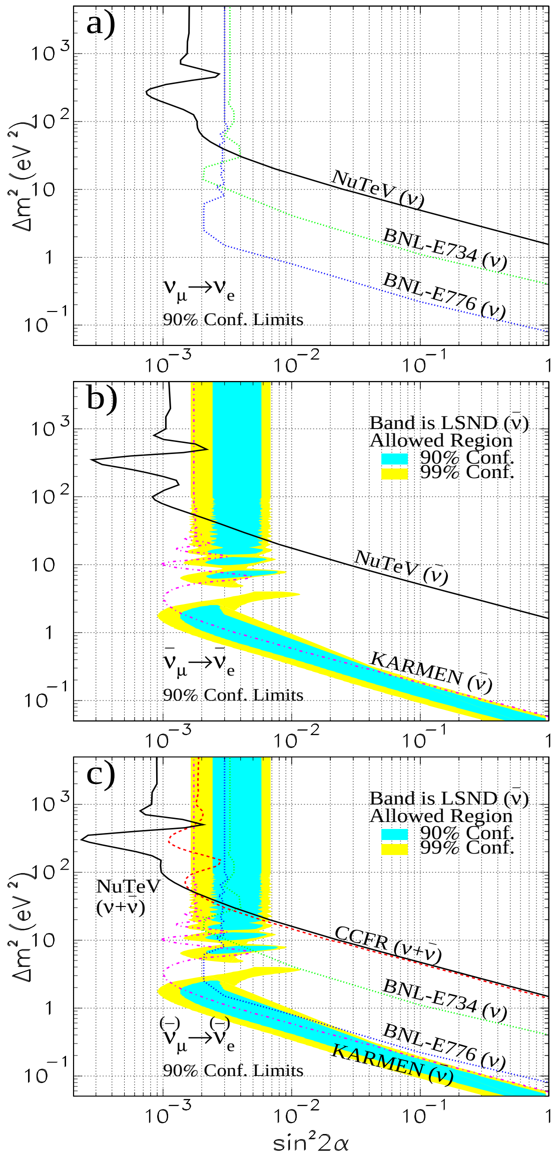

Figure 3: (a) Excluded region of $\sin^2 2\alpha$ and δm^2 for $\nu_\mu \to \nu_e$ oscillations from the NuTeV analysis at 90% confidence is the area to the right of the dark, solid curve. (b) NuTeV limits for $\overline{\nu}_\mu \to \overline{\nu}_e$. (c) Combined NuTeV limits for $\nu_\mu(\overline{\nu}_\mu) \to \nu_e(\overline{\nu}_e)$, assuming oscillation parameters for ν and $\overline{\nu}$ are the same.

3. Search for $\nu_\mu(\overline{\nu}_\mu)$ Oscillations

   S. Avvakumov, a Rochester PhD student on NuTeV (PhD 2002), extracted limits on $\nu_\mu \to \nu_e$ and $\overline{\nu}_\mu \to \overline{\nu}_e$ oscillations for his Ph.D. thesis. His thesis ,under the supervision of Professor Arie Bodek, was submitted in Jan 2002 . The results were published in PRL 89 011804,2002. (S. Avvakumov *et al.*, A search for $\nu_\mu \to \nu_e$ and $\overline{\nu}_\mu \to \overline{\nu}_e$ oscillations at NuTeV (hep-ex/0203018)).

   Since NuTeV had separate ν_μ and $\overline{\nu}_\mu$ beams, we search for oscillations in both running modes, without the need to assume that the oscillations parameters for neutrinos and antineutrinos are the same. The oscillations are searched for using a statistical separation of $\nu_e N$ charged current interactions in the NuTeV detector at Fermilab. The ν_e interactions are identified by the difference in the longitudinal shower energy deposition pattern of $\nu_e N \to eX$ versus $\nu_\mu N \to \nu_\mu X$ interactions. Using this technique, the absolute flux of ν_e's at the detector is measured and is compared to the flux predicted by a detailed beam line simulation. Any excess could be interpreted as a signal of $\nu_\mu \to \nu_e$ oscillations.

At all Δm^2, the data are consistent with no observed $\nu_\mu \to \nu_e$ oscillations. The frequentist approach is used to set a 90% confidence upper limit for each Δm^2. The limit in $\sin^2 2\alpha$ corresponds to a shift of 1.64 units in χ^2 from the minimum. The 90% confidence upper limit is shown in Fig. 3(a) for $\nu_\mu \to \nu_e$. Also shown are limits from BNL-E734 and BNL-E776. For $\sin^2 2\alpha = 1$, $\Delta m^2 > 2.4$ eV^2 is excluded, and for $\Delta m^2 \gg 1000$ eV^2, $\sin^2 2\alpha > 1.6 \times 10^{-3}$. In the large Δm^2 region, NuTeV provides improved limits for $\nu_\mu \to \nu_e$ oscillations.

Similarly, the limit for $\overline{\nu}_\mu \to \overline{\nu}_e$ is shown Fig. 3(b). Also shown are the LSND results and preliminary results from KARMEN. For the case of $\sin^2 2\alpha = 1$, $\Delta m^2 > 2.6$ eV^2 is excluded, and for $\Delta m^2 \gg 1000$ eV^2, $\sin^2 2\alpha > 1.1 \times 10^{-3}$. In the $\overline{\nu}_\mu$ mode, our results exclude the high Δm^2 end of $\overline{\nu}_\mu \to \overline{\nu}_e$ oscillations parameters favored by the LSND experiment, without the need to assume that the oscillation parameters for ν and $\overline{\nu}$ are the same. These are the most stringent experimental limits for $\nu_\mu(\overline{\nu}_\mu) \to \nu_e(\overline{\nu}_e)$ oscillations in the large Δm^2 region.

If we assume that the oscillation parameters for ν and $\overline{\nu}$ are the same, we can combine our ν and $\overline{\nu}$ results and compare to the CCFR results with a mixed beam. The combined NuTeV results exclude $\nu_\mu(\overline{\nu}_\mu) \to \nu_e(\overline{\nu}_e)$ oscillations with $\sin^2 2\alpha > 0.9 \times 10^{-3}$ for large $\Delta m^2 \gg 1000$ eV^2. For $\sin^2 2\alpha = 1$, $\Delta m^2 > 2.2$ eV^2 is excluded. These are the most stringent experimental limits for $\nu_\mu(\overline{\nu}_\mu) \to \nu_e(\overline{\nu}_e)$ oscillations in the large Δm^2 region.

Neutrino Oscillations and Electron and Neutrino Scattering at Low Energies

Arie Bodek, Howard Budd, Kevin McFarland (in collaboration with Prof. Steve Manly)

The recent discoveries of neutrino oscillations in atmospheric neutrinos [3] and in neutrinos from the sun [4, 5] motivate the detailed studies of neutrino oscillations at future high intensity neutrino beams from accelerators. The two disparate mass scales observed in oscillations from these astrophysical sources, $\delta m^2{}_{\mathrm{atm}} \approx 2 \times 10^{-3}$eV^2 and $\delta m^2{}_{\mathrm{solar}} \sim 10^{-4}$eV^2, along with the stringent limits on $\overline{\nu}_e$ disappearance at the atmospheric L/E in the CHOOZ and Palo Verde reactor experiments experiments[7, 8], have raised the possibility that there may be an observable CP-asymmetry in $\nu_\mu \to \nu_e$ transitions. This rare, sub-leading transition in the neutrino flavor sector is analogous to to searching for first and third generation mixing in the quark sector, which has led to a rich phenomenology of CP-violation, meson mixing and rare decays in the quark sector.

These neutrino oscillation experiments are very challenging, because of the required L/E of 400 km/GeV, and require megawatt proton sources, 1 GeV neutrino

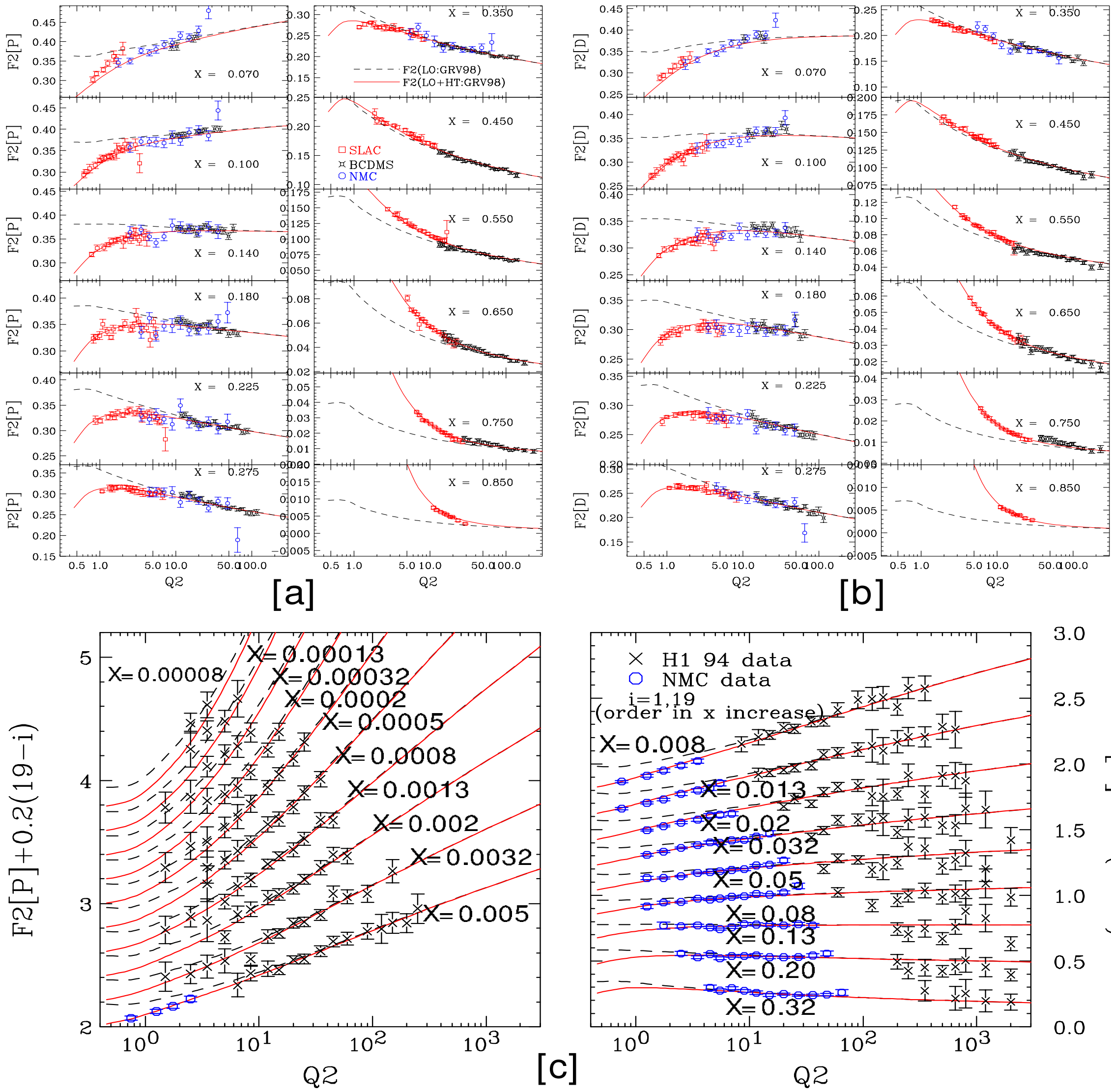

Figure 4: Electron and muon F_2 data (SLAC, BCDMS, NMC, H1 94) used to obtain the parameters of the Bodek-Yang modified GRV98 ξ_w fit compared to the predictions of the unmodified GRV98 PDFs (LO, dashed line) and the modified GRV98 PDFs fits (LO+HT, solid line); [a] for F_2 proton, [b] for F_2 deuteron, and [c] for the H1 and NMC proton data at low x.

beams and multi-kiloton detectors to make the observations. The measurements are further complicated by the low transition probability of $\nu_\mu \to \nu_e$ and the need to compare to $\overline{\nu}_\mu \to \overline{\nu}_e$ at high precision. This requires a detailed knowledge of the neutrino interaction cross-sections both for the dominant signal processes and for background processes, such as $\nu N \to \nu N \pi^0$ where the π^0 is misidentified as an electron in a many kiloton sampling detector.

Modeling Electron and Neutrino Scattering at Low Energies in the Continuum Region

A. Bodek (in collaboration with U. K. Yang)

The phenomenology of neutrino cross-sections is relatively simple when $E\nu \ll$ 1 GeV or when $E\nu \gg$ few GeV since these regimes are dominated by (quasi)-elastic and deep inelastic processes, respectively. However in the 1 to few GeV region, there are contributions to the cross-section from both of these processes as well as resonance-dominated hadroproduction. A successful phenomenological approach to modeling the resonance region in electron scattering is the use of quark-hadron duality to relate quark-model cross-sections to the cross-section over the discrete resonances [9] as shown in Fig. 4, Fig. 5 and Fig. 6. Figure 4 shows a fit by Bodek and Yang to inelastic electron and muon scattering data with a modified scaling variable and GRV98 PDFs with additional corrections (based on consideration of the Adler and Gilman sum rules [15]. Figure 5 and Figure 6 compare the predictions of the fit to data in the resonance region (which is not included in the fit, as well as other data such a photoproduction and high energy neutrino data). All predictions assume quark-model relations, and an empirical fit to R (R_{1998}). This approach requires the separation of the F_2, which has a simple representation in the quark model, and R whose description requires a different prescription. We plan to build successful models of neutrino scattering using this same prescription with the addition of a quark-model representation of the axial vector component of the cross-section.

Since neutrino data are measured in nuclear targets, even in the quark model case, the separated vector structure functions from electron scattering, F_{2p}, F_{2n}, R_p, R_n for bound nucleons are needed in order to understand the axial structure function in neutrino scattering experiments.

Modeling Electron and Neutrino Scattering at Low Energie in the Resonance Region

Work to be done in collaboratin with Cynthia Keppel of Hampton University and Jefferson Laboratory.

In addition to our investigation of the inelastic continuum we plan to used new precise data from Jefferson Lab to also do a combined analysis of electron-nucleon and neutrino nucleon data in the resonance region within the Feynman quark-oscillator model as done years ago (with poor precision) by Rein and Seghal [10]. The results of the updated Rein-Seghal type of analysis will be compared to an analysis which is based on duality.

The full program of studies will use precise electron scattering data, in particular σ_L and σ_T (or equivalenty F_2 and R) on Hydrogen and Deuterium. These studies will later be supllemented with data on nuclear targets targets (materials suited for future neutrino oscillation detectors – water [11], hydrocarbons [12], liquid argon – and steel, where the most precise high energy neutrino cross-sections have been measured [13]) in the relevant kinematic regime. Later, as the new generation of high rate neutrino beams at Fermilab and J-PARC become available, the approach can be directly validated with comparisons to data from high rate neutrino cross-section experiments on the same targets [14].

Modeling Quasi-elastic Form Factors for Electron and Neutrino Scattering

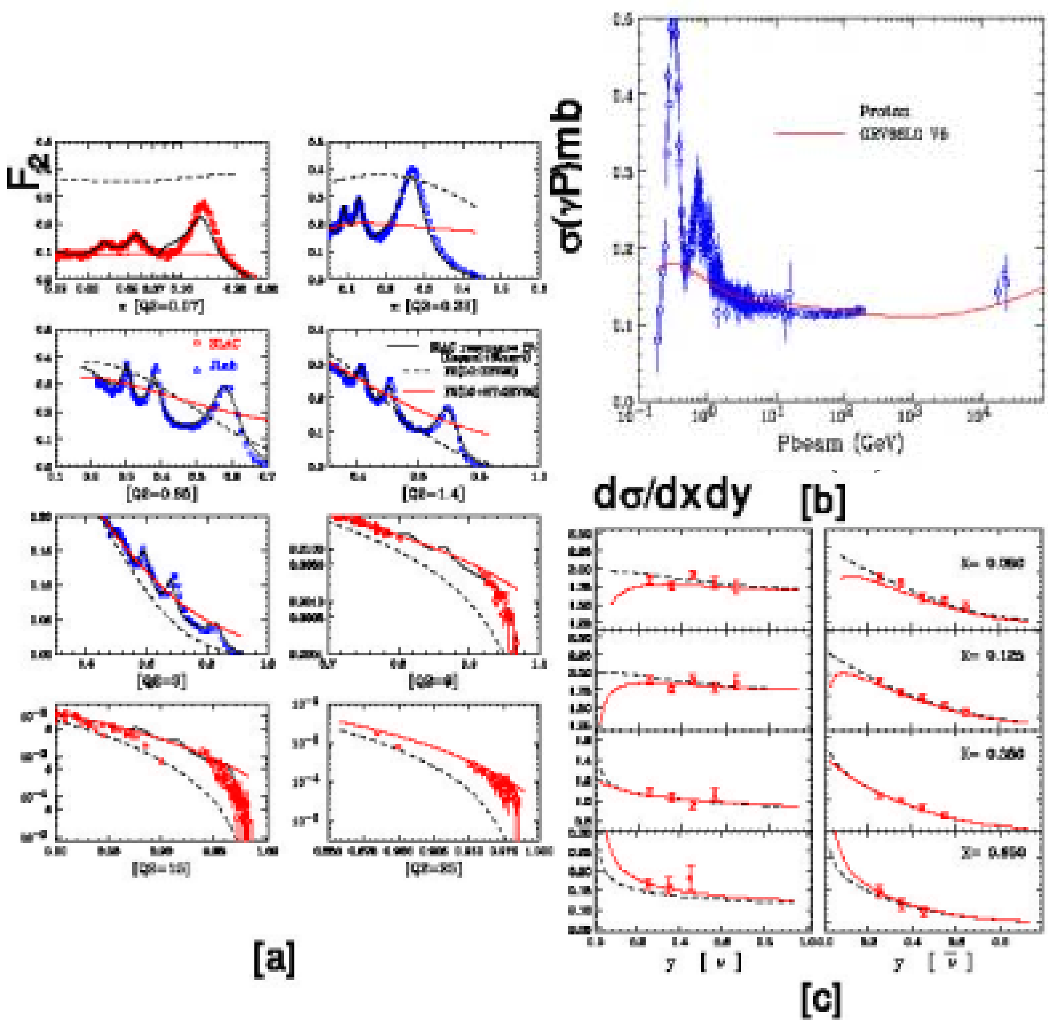

Figure 5: Comparisons to proton and iron data not included in the Bodek-Yang GRV98 ξ_w fit. (a) Comparison of SLAC and JLab (electron) F_{2p} data in the resonance region (or fits to these data) and the predictions of the GRV98 PDFs with (LO+HT, solid) and without (LO, dashed) the Bodek-Yang modifications. (b) Comparison of photoproduction data on protons to predictions using Bodek-Yang modified GRV98 PDFs. (c) Comparison of representative CCFR ν_μ and $\overline{\nu}_\mu$ charged-current differential cross sections on iron at 55 GeV and the predictions of the GRV98 PDFs with (LO+HT, solid) and without (LO, dashed) Bodek-Yang modifications.

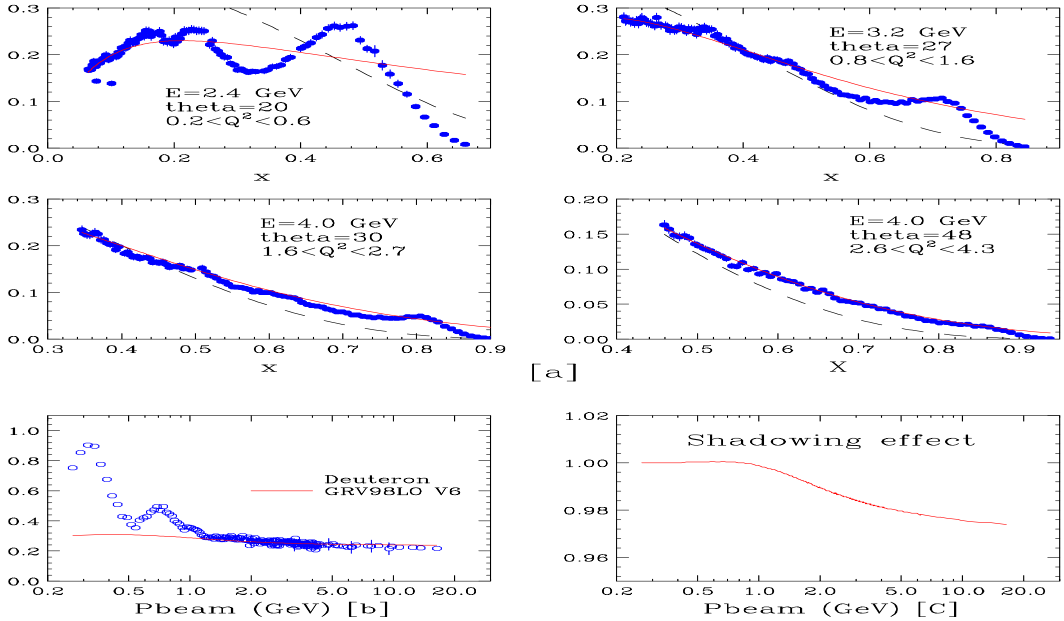

Figure 6: Comparisons to data on deuterium which were not included in the Bodek-Yang GRV98 ξ_w fit. (a) Comparison of SLAC and JLab (electron) F_{2d} data in the resonance region and the predictions of the GRV98 PDFs with (LO+HT, solid) and without (LO, dashed) our modifications. (b) Comparison of photoproduction data on deuterium to predictions using Bodek-Yang modified GRV98 PDFs (including shadowing corrections). (c) The shadowing corrections that were applied to the PDFs for predicting the photoproduction cross section on deuterium.

Arie Bodek, Howard Budd (in Collaboration with John Arrington of Argonne National Laboratory).

Since Quasielastic scattering forms an important component of neutrino scattering at low energies, we have undertaken to investigate QE neutrino scattering using the latest information.

Recent experiments at SLAC and Jefferson Lab (JLAB) have given very precise measurements of the vector electro-magnetic form factors for the proton and the neutron. These form factors can be related to the form factors for QE neutrino scattering by conserved vector current hypothesis, CVC. These more recent form factors can be used to give better predictions of QE scattering.

The hadronic current for QE neutrino scattering is given by

$$< p(p_2)|J_\lambda^+|n(p_1) >= \overline{u}(p_2)\left[\gamma_\lambda F_V^1(q^2) + \frac{i\sigma_{\lambda\nu}q^\nu\xi F_V^2(q^2)}{2M} + \gamma_\lambda\gamma_5 F_A(q^2) + \frac{q_\lambda\gamma_5 F_P(q^2)}{M}\right]u(p_1)$$

We do not include second class currents, so the scaler form factor F_V^3 and the tensor form factor F_A^3 are not included. Using the above current, the cross section is

$$\frac{d\sigma^{\nu,\ \overline{\nu}}}{dq^2} = \frac{M^2G_F^2cos^2\theta_c}{8\pi E_\nu^2}[A(q^2) \mp \frac{(s-u)B(q^2)}{M^2} + \frac{C(q^2)(s-u)^2}{M^4}],$$

where

$$A(q^2) = \frac{m^2 - q^2}{4M^2}\left[\left(4 - \frac{q^2}{M^2}\right)|F_A|^2 - \left(4 + \frac{q^2}{M^2}\right)|F_V^1|^2 - \frac{q^2}{M^2}|\xi F_V^2|^2\left(1 + \frac{q^2}{4M^2}\right) - \frac{4q^2 Re F_V^{1*}\xi F_V^2}{M^2}\right],$$

$$B(q^2) = -\frac{q^2}{M^2} Re F_A^*(F_V^1 + \xi F_V^2),$$

$$C = \frac{1}{4}\left(|F_A|^2 + |F_V^1|^2 - \frac{q^2}{M^2}\left|\frac{\xi F_V^2}{2}\right|^2\right).$$

We have not shown terms in $(m_l/M)^2$, and $F_P(q^2)$ is multiplied by $(m_l/M)^2$. (Note, $F_P(q^2)$ is included in the calculations.) The formulas for $F_V^1(q^2)$ and $cF_V^2(q^2)$ are

$$F_V^1(q^2) = \frac{G_E^V(q^2) - \frac{q^2}{4M^2}G_M^V(q^2)}{1 - \frac{q^2}{4M^2}}, \quad \xi F_V^2(q^2) = \frac{G_M^V(q^2) - G_E^V(q^2)}{1 - q^2/4M^2}$$

We use the CVC to determine $G_E^V(q^2)$ and $G_M^V(q^2)$ from the electron scattering form factors $G_E^p(q^2)$, $G_E^n(q^2)$, $G_M^p(q^2)$, and $G_M^n(q^2)$.

$$G_E^V(q^2) = G_E^p(q^2) - G_E^n(q^2), \quad G_M^V(q^2) = G_M^p(q^2) - G_M^n(q^2)$$

Many of the neutrino experiment have assumed the form factors are the dipole approximation.

$$G_D(q^2) = \frac{1}{(1 - q^2/M_V^2)^2}, \quad M_V^2 = 0.71\ GeV^2$$

$$G_E^p = G_D(q^2), \quad G_E^n = 0, \quad G_M^p = \mu_p G_D(q^2), \quad G_M^n = \mu_n G_D(q^2)$$

The axial form factor is given by

$$F_A(q^2) = \frac{g_A}{(1 - \frac{q^2}{M_A^2})^2}$$

This form factor needs to be determined from QE neutrino scattering. Older experiments used $g_A = -1.23$, however the current value is -1.267. The world average from neutrino experiments is $M_A = 1.026 \pm 0.02$ GeV. The value of M_A depends on the electro-magnetic form factors. Since we are updating these form factors, we need to determine a new value of M_A using these latest form factors and g_A. M_A can also be determined from pion electro-production, which gets 1.069 $\pm$ 0.016 GeV (it is expected that this determination is not as reliable as that from neutrino data because of theoretical corrections. These corrections bring the value into closer agreement with the value as measured in neutrino reactions).

From PCAC, the pseudoscaler form factor F_P is

$$F_P(q^2) = \frac{2M^2 F_A(q^2)}{M_\pi^2 - q^2}.$$

$F_P(q^2)$ is multiplied by $(m_l/M)^2$ so its effect is very small except at very low energy, $< .2GeV$.

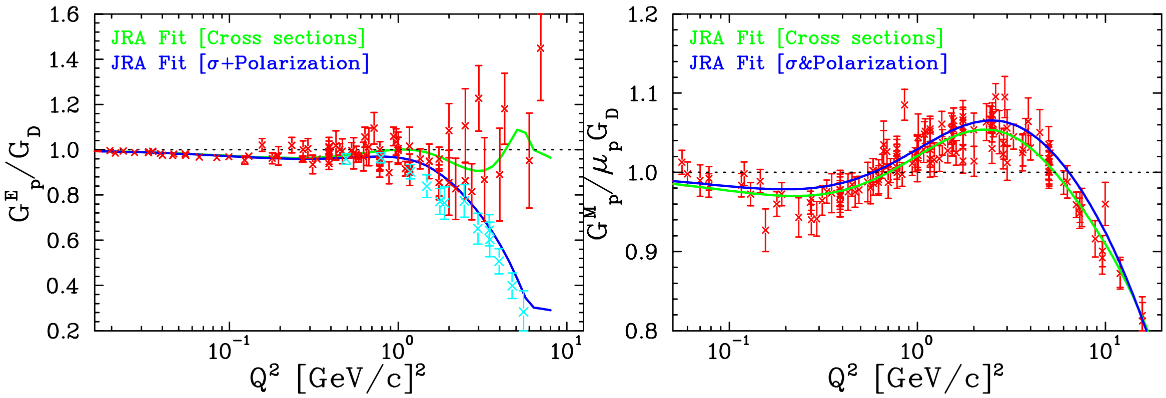

Figure 7: Our fits for G_E^p/G_D and $G_M^p/\mu_p G_D$. The fits with and without the polarization measurements are shown. Polarization data is shown in cyan.

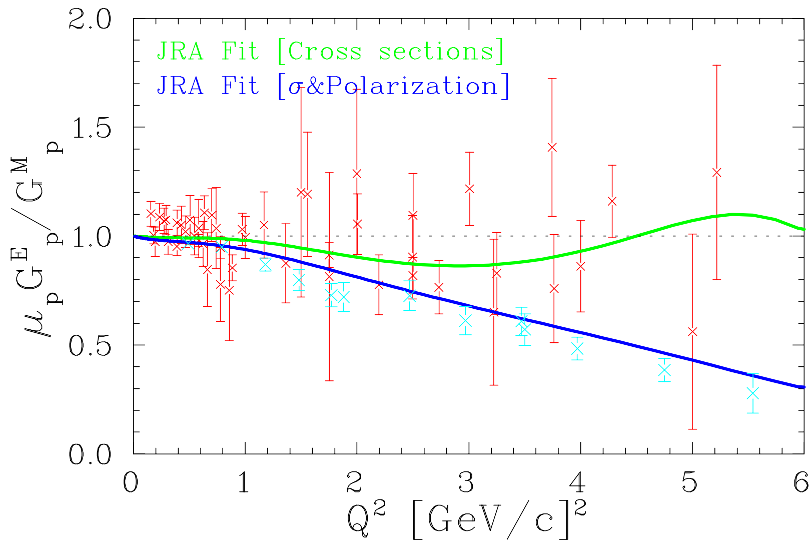

Figure 8: Ratio of G_E^p to G_M^p as extracted by Rosenbluth measurements and from polarization measurements.

We have used almost all data from SLAC and JLAB to determine the form factors. Form factors can be determined by using older technique of Rosenbluth separation (cross section) or the newer technique of polarization transfer from JLAB. Figure 7 shows the ratio of our fits divided by the dipole, G_D. The JLAB polarization measurement does not directly measure the form factors, but measures the ratio G_E^p/G_M^p. As we see from figure 8, G_E^p/G_M^p is flat vs Q^2 ($Q^2 = -q^2$) for the cross section measurement. However, G_E^p/G_M^p decreases for the polarization measurement. Although the polarization measurement is believed to have smaller systematic error especially at high Q^2, the origin of this disagreement is not known. Experiments at JLAB hope to resolve this disagreement.

	a_2	a_4	a_6	a_8	a_{10}	a_{12}
G_E^p	3.253	1.422	0.08582	0.3318	-0.09371	0.01076
G_M^p	3.104	1.428	0.1112	-0.006981	0.0003705	-0.7063E-05
G_M^n	3.043	0.8548	0.6806	-0.1287	0.008912	

Table 1: The coefficients of the inverse polynomial for the G_E^p, G_M^p, and G_M^n. This fit uses both cross section data and polarization data from electron scattering.

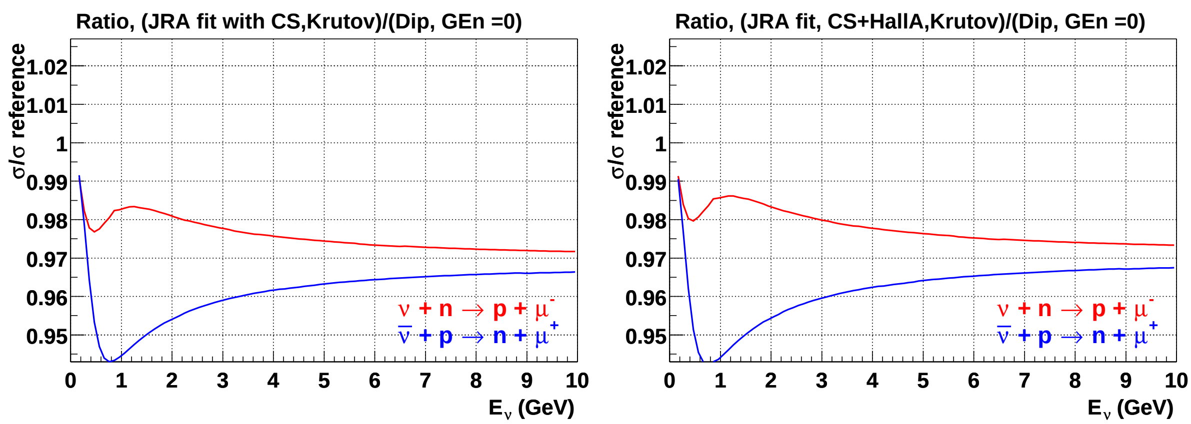

Figure 9: Ratio of cross section vs energy using the most updated form factors vs the dipole approximation. The left plot uses the Rosenbluth separation data and the polarization data. The right plot uses Rosenbluth separation data.

We fit electron scattering data to an inverse polynomial

$$Poly^{-1}(Q^2) = \frac{1}{1 + a_2 Q^2 + a_4 Q^4 + a_6 Q^6 + \ldots}.$$

Table 1 shows the results of our fit. These fits uses both cross section data and polarization transfer data from JLAB. In addition, we have fits which just use the cross section data.

Previous experiments assumed $G_E^n(q^2) = 0$. Since the neutron has no charge, $G_E^n(q^2)$ must be zero at $q^2 = 0$. However, it doesn't have to zero for $q^2 \neq 0$. New JLAB polarization transfer data gives a precise non-zero value of $G_E^n(q^2)$. Our analysis uses $G_E^n(q^2)$ from Krutov et. al. (Hep-ph/0202183).

$$G_E^n = -\mu_n \frac{a\tau}{1 - b\tau} G_D(q^2), \quad \tau = \frac{Q^2}{4M^2}.$$

Figure 9 shows the ratio of the QE cross section using the most updated form factors vs the dipole approximation. The most updated form factor are our fits to the form factors for G_M^p, G_E^p, and G_M^n and Krutov G_E^n. The left plot uses the cross section data and the polarization data. The right plot uses Rosenbluth separation

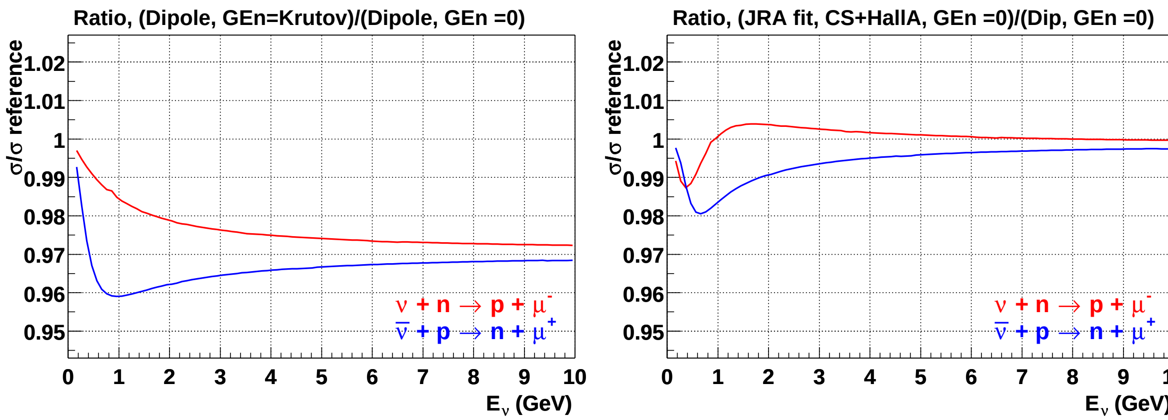

Figure 10: Ratio of cross section vs energy using different sets of form factors vs energy. The left plot looks at the difference between using G_E^n = Kurtov vs $G_E^n = 0$. The right plots looks at the difference between using our fits for G_E^p, G_M^p, and G_N^n vs the dipole approximation.

data. The cross section for neutrino QE scattering is independent of the polarization data. The differences between the polarization data and the cross section data are at high Q^2, while the form factors contribute to the cross section at low Q^2.

There is a big effect in the cross section between using the latest form factors or not. The difference is 3% at high energy and can become as much as 6% at 1 GeV. Figure 9 shows the difference between G_E^n = Krutov vs $G_E^n = 0$. We see all of the difference at high energy and most of the the difference at low energy is due to G_E^n. At low energy, which are the energies for neutrino oscillation experiments, the other form factors are important.

A 1% increase in either M_A or $|g_A|$ increases the cross section about 1%. As the old value of g_A=-1.23. and more recent values of -1.267 increases the cross section by about 2.5%. In addition the more recent value of M_A of 1.02 vs the 1.032 causes the cross section to fall by about 1%. M_P has almost no effect on the cross section except at very low E_ν.

Previous neutrino experiment, mostly bubble chambers, extract M_A using the best known assumptions at the time. Changing these assumptions changes M_A. Hence, we use published data to extract a corrections to M_A using our form factors. They give their data in histograms of corrected events. Their flux is shown in figures, which we parameterize using a spline fit. We calculate the Q^2 distribution of their data and fit their data for M_A. We determine M_A using their assumptions and our assumptions. Figure 11 shows a histograms of the Q^2 distribution for both Baker et. al. and Kitagaki et. al. Our curves agree very well with their curves. In addition our curves agree very well with Barish et al, but not quite so well with Miller et al. As Miller gives the final result of Barish, adding 3 times the data, they should be using the same code. Therefore, the discrepency between Miller and Barish is puzzling.

We fit for M_A using their assumptions and our assumptions, and we determine

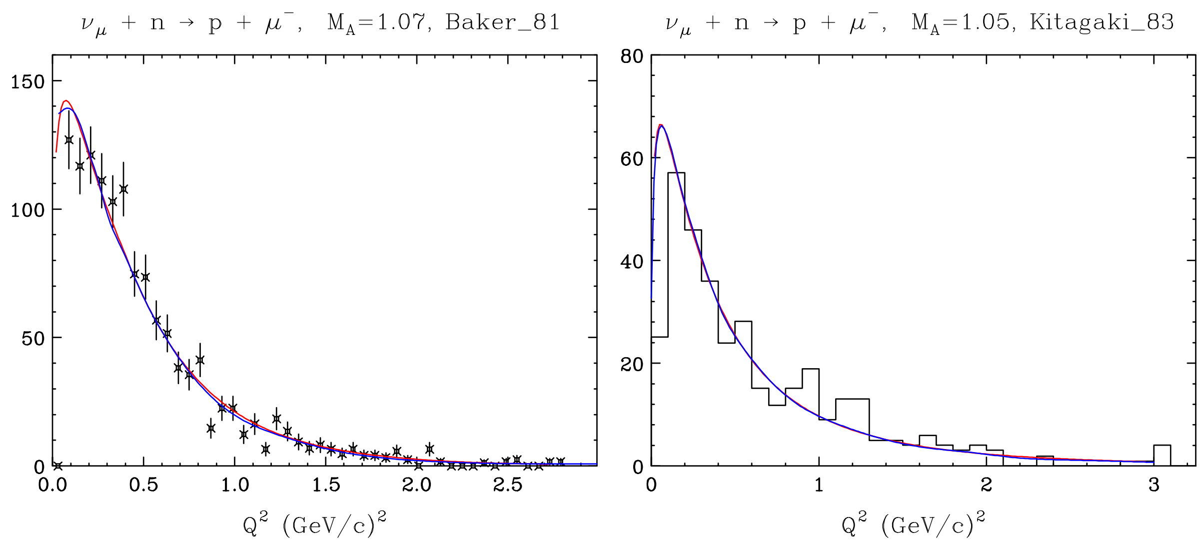

Figure 11: Q^2 distribution from Baker et. al. and Kitagaki et. al. The red curve is our calculation using their assumptions. The blue curve is their calculation taken from their Q^2 distribution histogram.

the shift using our assumption. They calculate M_A using unbinned maximum likelihood, which we can't do since we do not have the events. We use binned maximum likelihood. These experiment use a dipole correction from Ollson et. al. [PRD 17 2938 (1978)]. Table 2 gives the result of the calculation. We also determine M_A using the dipole. We agree with the value of M_A of Baker, but disagree with the values of Barish, Miller, and Kitagaki. However, as previously stated our Q^2 distributions agree very well with Baker, Barish, and Kitagaki. Maybe their unbinned likelihood fit as opposed to our binned likelihood fit creates the difference. But then why did we get Baker's value correct? We do not have an explanation for the discrepency in M_A. The table indicates we should shift the value of M_A determined from deuterium down by 0.025 GeV.

Figure 12 shows the QE cross section for ν and $\overline{\nu}$ using our most up to date assumptions. We have used form factors from cross section and polarization measurements. We used G_A = -1.267. We have scaled down M_A from the old best fit of M_A=1.026 ± 0.021 to M_A=1.00 (which would have been obtained with the best vector form factors known today). Even with the most up to date assumptions on form factors the agreement between data and predicction is not spectacular. The data - flux errors are 10%. The anti-neutrino data, which is on nuclear targets, is below the curves. This is most likely due to nuclear physics effects. Over the next year, we plan to study the nuclear corrections (using models which work in electron scattering). In addition, we wil be calculating the corrections to the M_A values for other experiments (to update the results for the latest vector form factors).

	Their Fit	Our Fit Their Assum.	Our Assum.	Our - Their δM_A	Our - Dipole δM_A
Barish 77	1.01 ± 0.09	1.087 ± 0.10	1.058	-0.029	-0.048
Miller 82	1.05 ± 0.05	1.118 ± 0.055	1.091	-0.027	-0.046
Kitagaki 83	$1.05^{+0.12}_{-0.16}$	1.139 ± 0.10	1.118	-0.021	-0.052
Baker 81	1.07 ± 0.06	1.075	1.050	-0.025	-0.049

Table 2: Fit values and shifted values of M_A (GeV) from deuterium experiments. Column 2 gives the fit values of M_A from their papers. For Barish and Miller, we give their "shape fit" value, since this value most closely reflects how we can calculate their M_A. Column 3 gives our fit value of M_A using their assumptions. Column 4 gives our fit value of M_A with our assumptions. Column 5 gives δM_A between our assumptions minus the experiments assumptions. Column 6 gives δM_A between using our form factors and a dipole form factors. For this difference the value of g_A is kept the constant.

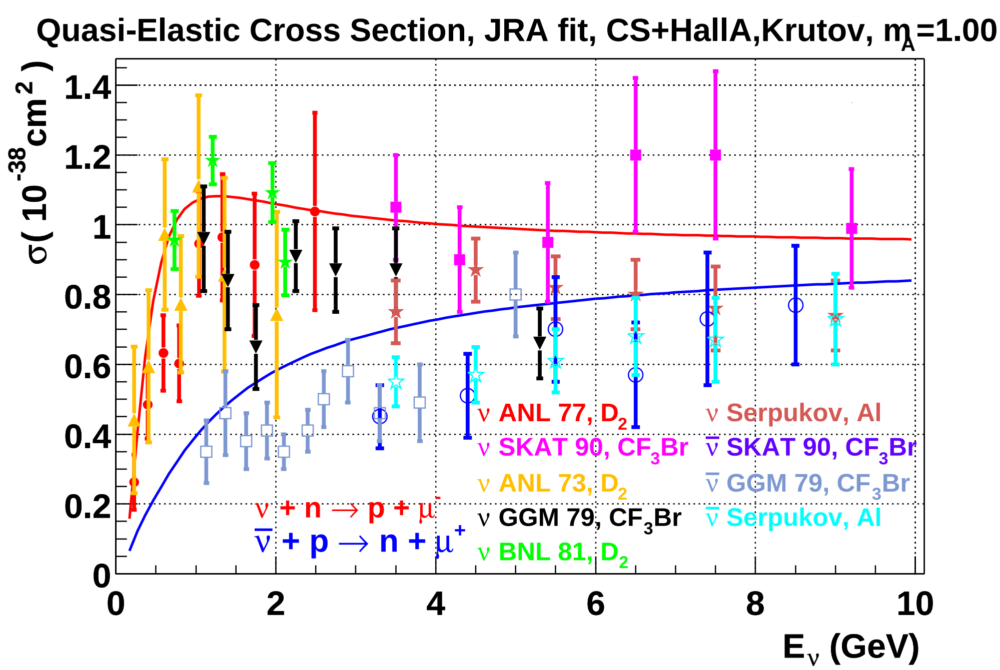

Figure 12: The QE cross section and ν and $\overline{\nu}$ along with data from various experiment. The calculation uses the latest form factors and M_A = 1.00 and G_A = -1.267

References

[1] SLAC Experiment E140, A. Bodek and S. Rock, Spokespersons; S. Dasu et al., Phys. Rev. Lett. 61, 1061 (1988); S. Dasu et al., Phys. Rev. D49, 5641 (1994) ; S. Dasu, Ph.D. Thesis, University of Rochester, 1988 (UR-1059).

[2] JLab experiment 99-118 on the nuclear dependence of R at low Q^2, A. Brull, C.E. Keppel spokespersons

(http://www.jlab.org/exp_prog/proposals/99/PR99-118.pdf)

[3] Y. Fukada *et al.*, Phys.Rev.Lett. 81 (1998) 1562.

[4] SNO Collaboration, nucl-ex/0204008, nucl-ex/0204009.

[5] K. Eguchi *et al.* [KamLAND Collaboration], Phys. Rev. Lett. **90**, 021802 (2003).

[6] A. Aguilar *et al.* [LSND Collaboration], anti-nu/e appearance in a anti-nu/mu beam," Phys. Rev. D **64**, 112007 (2001).

[7] M. Apollonio *et al.*, Phys.Lett. **B466** (1999) 41.

[8] F. Boehm *et al.*, Nucl.Phys.Proc.Suppl. 91 (2001).

[9] A. Bodek and U. K. Yang, hep-ex/0203009, Nucl.Phys.Proc.Suppl.112:70-76,2002.
A. Bodek and U. K. Yang, hep-ex/0301036.
A. Bodek, U. K. Yang, hep-ex/0210024, J. Phys. G. Nucl. Part. Phys.,**29**, 1 (2003). These were based on previous work by Bodek and Yang including studies in NLO +TM +HT (Phys. Rev. Lett 82, 2467 (1999) ; Phys. Rev. Lett. 84, 3456 (2000)) and studies in NNLO +TM +HT (Eur. Phys. J. C13, 241 (2000))

[10] D. Rein and L. M. Sehgal, Annals Phys. **133** 79 (1981) ;D. Rein, Z. Phys. C. 35, 43 (1987); R. P. Feynman, M. Kislinger and F. Ravndal, Phys. Rev. D**3**, 2706 (1971); and R. Belusevic and D. Rein, Phys. Rev. D **46**, 3747 (1992).

[11] Y. Itow *et al.*, "The JHF-Kamioka Neutrino Project", hep-ex/0106019.

[12] http://www-numi.fnal.gov/fnal_minos/new_initiatives/new_initiatives.html

[13] U. K. Yang *et al.*(CCFR), Phys. Rev. Lett. **87**, 251802 (2001).

[14] http://home.fnal.gov/~dharris/xsec_agenda.html

[15] S. L. Adler, Phys. Rev.**143**, 1144 (166); F. Gilman, Phys. Rev. **167**, 1365 (1968).